Angewandte Chemie
Eine Zeitschrift der Gesellschaft Deutscher Chemiker

Supporting Information

69451 Weinheim, Germany

SUPPORTING INFORMATION

Porphyrin Dimer Carbocations with Strong Near Infrared Absorption and Third-Order Optical Nonlinearity

Karl J. Thorley[a], Joel M. Hales[b], Harry L. Anderson [a,]* and Joseph W. Perry[b,]*

[a]Contribution from the Chemistry Research Laboratory, Department of Chemistry, University of Oxford, Mansfield Road, Oxford OX1 3TA, United Kingdom and the [b]School of Chemistry and Biochemistry, Georgia Institute of Technology, Atlanta, Georgia 30332-0400

List of Contents

Section 1. Synthesis and Characterization.

Where applicable, solvents were deoxygenated by repeatedly reducing pressure and flushing with nitrogen or argon. Reactions were carried out under nitrogen or argon atmospheres, unless otherwise stated. Dry toluene and THF were obtained by passing through a column of activated alumina. All other reagents were used as supplied.

Column chromatography was carried out on silica gel 60 under a positive pressure of nitrogen. Where mixtures of solvents were used, ratios are reported by volume.

NMR spectra were recorded at ambient probe temperature, using a Brucker DPX400 (400 MHz) spectrometer. Spectra recorded on the Brucker AVANCE AVC500 (500 MHz) spectrometer were recorded by Dr. B. Odell. Chemical shifts are quoted as parts per million (ppm) relative to tetramethylsilane (0.00 ppm). Coupling constants (*J*) are quoted in Hertz (Hz). UV-Vis spectra were recorded in solution on a Perkin-Elmer lambda 20 UV-Vis spectrometer and UV-Vis-NIR spectra were recorded in solution on a JASCO V-570 spectrometer. Mass spectra were measured by Matrix Assisted Laser Desorption Ionisation – Time of Flight (MALDI-TOF) using a Micromass MALDI micro MX spectrometer. The matrix used for MALDI-TOF was dithranol (1,8,9-anthracenetriol). Only molecular ions and major peaks are given.

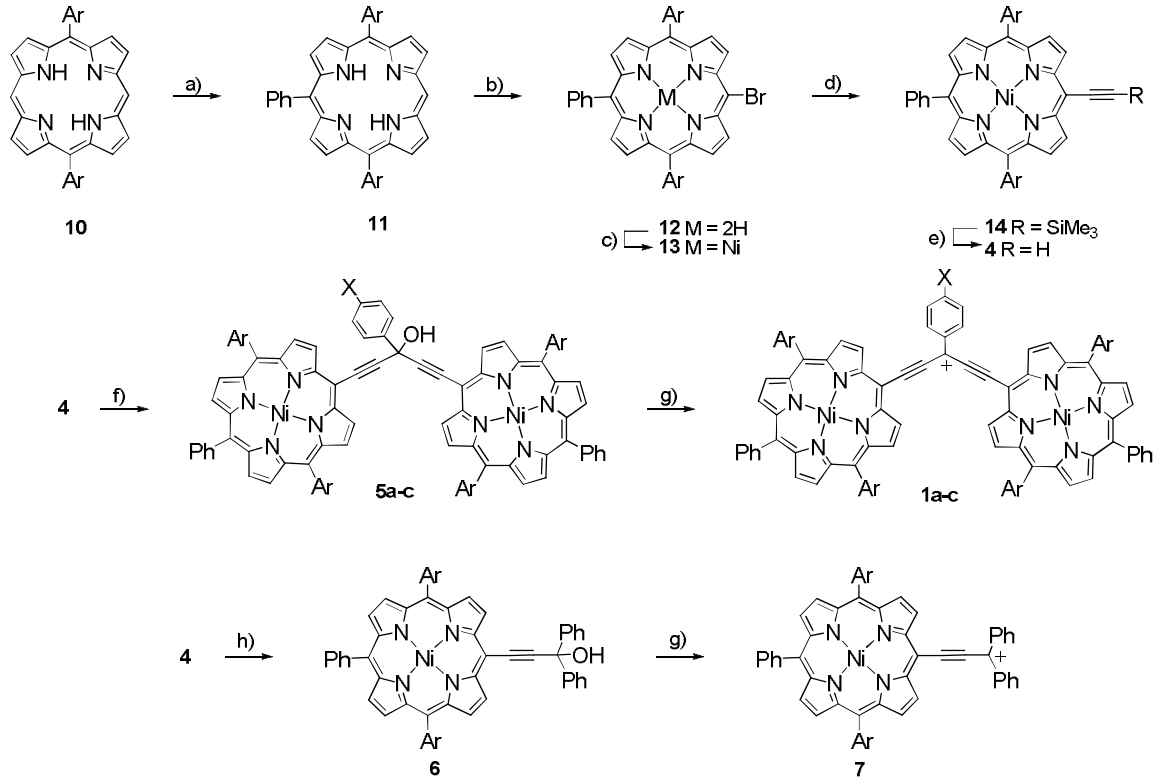

Scheme S1. Synthetic scheme to cationic porphyrins **1a** (X = H), **1b** (X = NO_2), **1c** (X = OMe) and **7**, Ar = 3,5-(*t*-Bu)$_2$C$_6$H$_3$. *Reagents and conditions;* a) i) PhLi, THF, 0°C; ii) H_2O, THF; iii) 2,3-dichloro-5,6-benzoquinone, CH_2Cl_2; b) *N*-bromosuccinimide; $CHCl_3$, pyridine, rt; c) $Ni(OAc)_2.4H_2O$, DMF, 150°C; d) Trimethylsilylacetylene, Pd_2dba_3, PPh_3, CuI, PhMe, NEt_3, 40°C; e) Bu_4NF, CH_2Cl_2; f) $XC_6H_4CO_2Me$, $LiN(SiMe_3)_2$, THF; g) CF_3CO_2H, $CHCl_3$; h) Ph_2CO, $LiN(SiMe_3)_2$, THF.

10-Phenyl-5,15-di(3,5-*t*-butyl phenyl) porphyrin **11**

Triaryl porphyrin **11** was synthesized by a procedure originally published by Senge.[1] To a solution of diaryl porphyrin **10** (0.100 g, 0.13 mmol) in dry THF (10 mL), phenyllithium (1.8 M in dibutylether, 0.72 mL, 1.3 mmol) was added at 0°C. The solution was stirred for 30 min at room temperature, before adding water (1 mL) to quench the reduced porphyrin anion and excess phenyllithium. The reaction mixture was poured into a solution of 2,3-dichloro-5,6-benzoquinone (0.118 g, 0.52 mmol) in CH_2Cl_2 (70 mL). After stirring for 10 min, the mixture was passed through a short silica plug. Removal of the solvents gave 10-phenyl-5,15-di(3,5-di-*t*-Bu phenyl) free base porphyrin **11** (0.095g, 83 % yield) as a purple solid. ^{1}H NMR (400 MHz, $CDCl_3$) δ 10.25 (1H, s), 9.37 (2H, d, *J* = 4.6 Hz), 9.12 (2H, d, *J* = 4.6 Hz), 8.99 (2H, d, *J* = 4.8 Hz), 8.92 (2H, d, *J* = 4.8 Hz), 8.26 (2H, d, *J* = 6.2 Hz), 8.17 (4H, d, *J* = 1.6 Hz), 7.86 (2H, t, *J* = 1.6 Hz), 7.74-7.82 (3H, m), 1.59 (36H, s), -2.88 (2H, s); ^{13}C NMR (100 MHz, $CDCl_3$) δ 149.0, 142.9, 140.8, 134.4, 130.1, 127.7, 126.5, 121.0, 120.3, 104.65, 35.12, 31.81; *m/z* (MALDI-TOF, +ve) 764.1 ($C_{54}H_{58}N_4$ requires 763.5).

10-Phenyl-5,15-di(3,5-di-*t*-Bu phenyl)-20-bromo free base porphyrin **12**

Bromoporphyrin **12** was synthesized by a modification of a published procedure.[2] To a solution of triaryl porphyrin **11** (0.325 g, 0.426 mmol) in $CHCl_3$ (34 mL) and pyridine (0.4 mL), a solution of *N*-bromosuccinimide (0.098 g, 0.554 mmol) in $CHCl_3$ (23 mL) and pyridine (0.25 mL) was added dropwise. The solution was stirred for 10 min at room temperature, and the reaction closely monitored by TLC (2:1 40-60 °C Petroleum ether / CH_2Cl_2). Acetone (4 mL) was added to quench the reaction. The reaction mixture was then passed through a short silica plug (CH_2Cl_2). The solvents were removed to give bromoporphyrin **12** (0.299 g, 83 % yield) as a purple solid. λ_{max} ($CHCl_3$) / nm (log ε) 423 (5.38), 521 (3.98), 556 (3.75), 598 (3.44), 653 (4.50); ^{1}H NMR (400 MHz, $CDCl_3$) δ 9.72 (2H, d, *J* = 4.7 Hz), 8.99 (2H, d, *J* = 4.7 Hz), 8.88 (2H, d, *J* = 4.6 Hz), 8.84 (2H, d, *J* = 4.6 Hz), 8.22 (2H, d, *J* = 6.9 Hz), 8.11 (4H, d, *J* = 1.6 Hz), 7.86 (2H, t, *J* = 1.6 Hz), 7.74-7.79 (3H, m), 1.58 (36H, s), -2.65 (2H, s). *m/z* (MALDI-TOF, +ve) 843.0 ($C_{54}H_{57}BrN_4$ requires 842.4)

10-Phenyl-5,15-di(3,5-di-*t*-Bu phenyl)-20-bromo nickel porphyrin **13**

Free base triaryl bromo-porphyrin **12** (0.290 g, 0.34 mmol) and $Ni(OAc)_2.4H_2O$ (0.429 g, 1.72 mmol) were dissolved in dimethylformamide (100 mL) and the solution brought to reflux. After stirring for 30 min at 150 °C, the reaction mixture was concentrated under high vacuum. The solid was redissolved in CH_2Cl_2 and then passed through a short silica plug (CH_2Cl_2). Removal of the solvent gave nickel porphyrin **13** (0.305 g, 99 % yield) as a red solid. λ_{max} ($CHCl_3$) / nm (log ε) 420 (5.12), 534 (3.98); ^{1}H NMR (400 MHz, $CDCl_3$) δ 9.55 (2H, d, *J* = 4.8 Hz), 8.89 (2H, d, *J* = 4.8 Hz), 8.79 (2H, d, *J* = 4.7 Hz), 8.76 (2H, d, *J* = 4.7 Hz), 8.03 (2H, d, *J* = 5.7 Hz), 7.90 (4H, d, *J* = 1.5 Hz), 7.79 (2H, t, *J* = 1.5 Hz), 7.69-7.72 (3H, m), 1.53 (36H, s); *m/z* (MALDI-TOF, +ve) 899.0 ($C_{54}H_{55}BrN_4Ni$ requires 898.3)

10-Phenyl-5,15-di(3,5-di-*t*-Bu phenyl)-20-(TMS acetylene) nickel porphyrin **14**

Acetylenic porphyrin **14** was synthesized by adapting an existing procedure.[3] Nickel triaryl-bromoporphyrin **13** (0.220 g, 0.245 mmol), copper(I) iodide (2.3 mg, 0.012 mmol), triphenylphosphine (6.4 mg, 0.025 mmol) and $Pd_2(dba)_3$ (11.2 mg, 0.012 mmol) were dried under vacuum in a two neck flask. The mixture was dissolved in dry toluene (15 mL) and freshly distilled triethylamine (4 mL). The solution was degassed using consecutive freeze-thaw-pump cycles. Trimethylsilyl acetylene (0.07 mL, 0.49 mmol) was added by syringe at room temperature. The reaction mixture was stirred at 40 °C for 3 hours. After completion of the reaction, the mixture was passed through a short silica plug (CH_2Cl_2). Following further purification by silica chromatography (3:1 40-60°C Petroleum ether / CH_2Cl_2), removal of solvents gave TMS acetylene porphyrin **14** (0.210 g, 93 % yield) as a purple solid. ^{1}H NMR (400 MHz, $CDCl_3$) δ 9.60 (2H, d, *J* = 4.8 Hz), 8.92 (2H, d, *J* = 4.8 Hz), 8.79 (2H, d, *J* = 4.7 Hz), 8.76 (2H, d, *J* = 4.7 Hz), 8.06 (2H, d, *J* = 5.4 Hz), 7.94 (4H, d, *J* = 1.6 Hz), 7.81 (2H, t, *J* = 1.6 Hz), 7.68-7.73 (3H, m), 1.56 (36H, s), 0.62 (9H, s) *m/z* (MALDI-TOF, +ve) 916.3 ($C_{59}H_{64}N_4NiSi$ requires 915.4).

10-Phenyl-5,15-di(3,5-di-*t*-Bu phenyl)-20-acetylene nickel porphyrin **4**

Deprotected acetylenic porphyrin **4** was made by a modification of a previously published procedure.[4] Trimethylsilyl protected acetylene porphyrin **14** (0.05 g, 0.055 mmol) was dissolved in CH_2Cl_2. Tetrabutylammonium fluoride (1.0 M in THF, 0.06 mL, 0.06 mmol) was added under N_2. After 10 min, calcium chloride (0.02 g) was added and the mixture stirred for a further 10 min. The mixture was then passed through a short silica plug (CH_2Cl_2). Removal of solvents gave the terminal acetylene porphyrin **4** as a red solid (0.046 g, 99 % yield) which was used as a reactant without delay. ^{1}H NMR (400 MHz, $CDCl_3$) δ 9.54 (2H, d, *J* = 4.8 Hz), 8.88 (2H, d, *J* = 4.8 Hz), 8.73 (2H, d, *J* = 4.8 Hz), 8.71 (2H, d, *J* = 4.8 Hz), 8.00 (2H, d, *J* = 7.6 Hz), 7.87 (4H, d, *J* = 1.6 Hz), 7.75 (2H, t, *J* = 1.6 Hz), 7.65-7.70 (3H, m), 4.07 (1H, s), 1.50 (36H, s).

NiC5 alcohol alkyne porphyrin dimer **5a** (X = H)

Porphyrin dimer **5a** was synthesized by adapting a known procedure.[5] Acetylene porphyrin **4** (0.063 g, 0.075 mmol) was dissolved in dry THF (1.5 mL) and cooled to −78°C. Lithium bis(trimethylsilyl)amide (1.0 M in THF, 0.30 mL, 0.30 mmol) was added to the porphyrin solution, immediately followed by methyl benzoate (5.0 µL, 0.037 mmol). The reaction mixture was allowed to warm to room temperature and stirred for 1 hr, after which the reaction was quenched with aqueous ammonium chloride (1 mL). The product was extracted with CH_2Cl_2 (30 mL) and washed with H_2O (3 × 20 mL), before passing through a short silica plug (CH_2Cl_2). The product was purified by column chromatography (2:1 40-60°C Petroleum ether / CH_2Cl_2). Removal of the solvent gave the product **5a** as a red solid (0.030 g, 53 % yield). λ_{max} ($CHCl_3$) / nm (log ε) 431 (5.62), 542 (4.57), 576 (4.37); ^{1}H NMR (400 MHz, $CDCl_3$) δ 9.66 (4H, d, *J* = 4.8 Hz), 8.85 (4H, d, *J* = 4.8 Hz), 8.74 (4H, d, *J* = 4.8 Hz), 8.72 (4H, d, *J* = 4.8 Hz), 8.62 (2H, d, *J* = 7.9 Hz), 8.02 (4H, d, *J* = 5.7 Hz), 7.86 (8H, s), 7.67-7.73 (14H, m), 7.60 (1H, t, *J* = 7.9 Hz), 3.83 (1H, s), 1.46 (72H, s). ^{13}C NMR (125 MHz, $CDCl_3$) δ 149.0, 145.1, 143.6, 142.8, 142.7, 142.5, 140.8, 139.5, 133.7, 133.6, 132.4, 132.3, 131.3, 129.1, 128.8, 127.8, 126.9, 126.4, 121.3, 121.2, 120.6, 96.9, 96.1, 86.6, 67.6, 35.0, 31.7; *m/z* (MALDI-TOF, +ve) 1775.7 (100%), 1792.8 (35%) ($C_{119}H_{116}N_8Ni_2O$ requires 1791.8, -OH requires 1774.8).

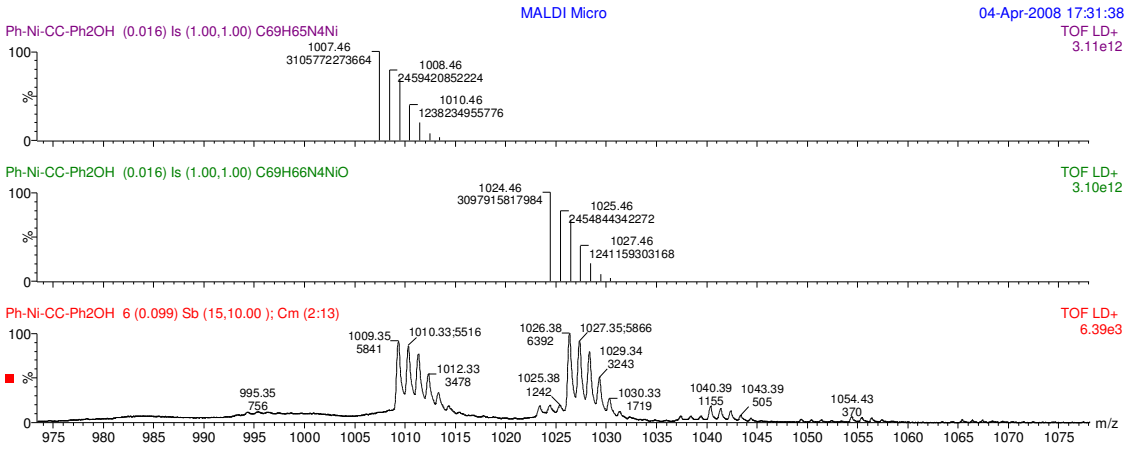

Figure S1. MALDI-TOF spectrum of porphyrin dimer **5a**, using a dithranol matrix. Calculated isotopic patterns of dimer **5a** (middle) and cation **1a** (top) are included for reference

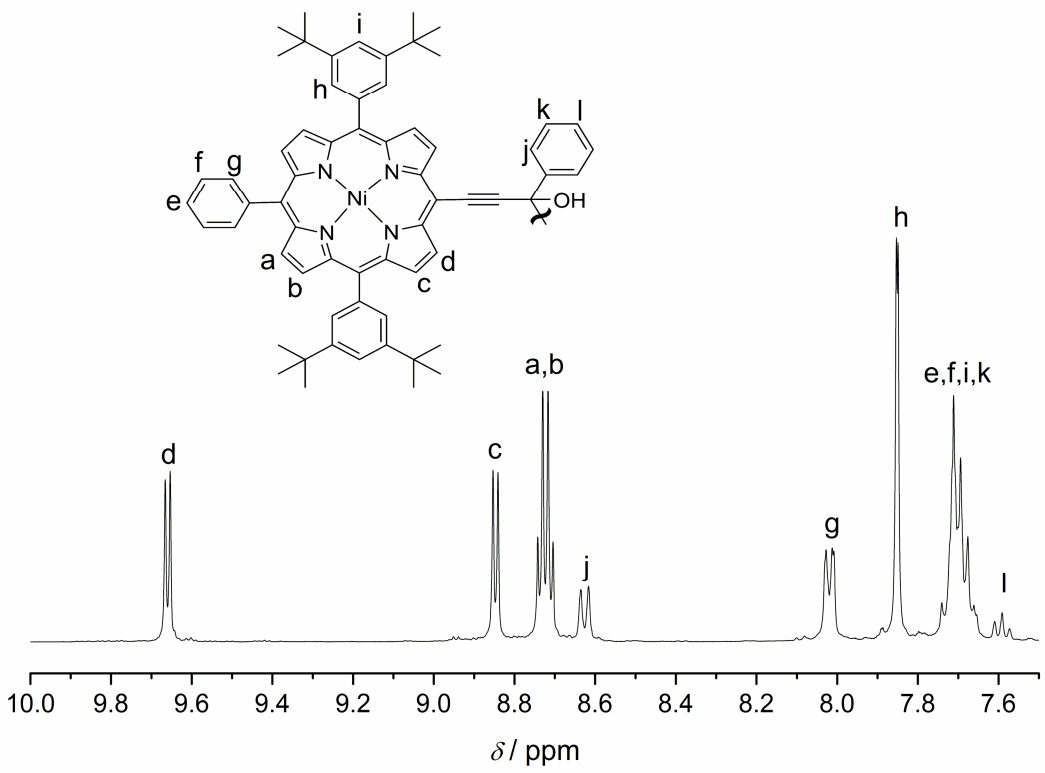

Figure S2. Aromatic region of 400 MHz ^{1}H NMR spectrum of porphyrin dimer **5a** recorded in $CDCl_3$ at 298 K

5b (X = NO_2)

Nitro substituted dimer **5b** was synthesized by a similar procedure as that for **5a**. Acetylene porphyrin **4** (0.050 g, 0.059 mmol) and methyl *p*-nitrobenzoate (0.0053 g, 0.03 mmol) were dissolved in dry THF (1 mL) and cooled to −78°C. Lithium bis(trimethylsilyl)amide (1.0 M in THF, 0.24 mL, 0.24 mmol) was added to the above solution. The reaction mixture was allowed to warm to room temperature and stirred for 1 hr, after which the reaction was quenched with aqueous ammonium chloride (1 mL). The product was extracted with CH_2Cl_2 (30 mL) and washed with H_2O (3 × 20 mL), before passing through a short silica plug (CH_2Cl_2). The product was purified by column chromatography (2:1 40-60°C Petroleum ether / CH_2Cl_2). Removal of the solvent gave the product **5b** as a red solid (0.032 g, 60 % yield). λ_{max} ($CHCl_3$) / nm (log ε) 430 (5.60), 543 (4.55), 577 (4.38); ^{1}H NMR (400 MHz, $CDCl_3$) δ 9.56 (4H, d, *J* = 4.9 Hz), 8.83 (4H, d, *J* = 4.9 Hz), 8.77 (2H, d, *J* = 8.9 Hz), 8.71 (8H, m), 8.56 (2H, d, *J* = 8.9 Hz), 8.00 (4H, d, *J* = 6.0 Hz), 7.83 (8H, d, *J* = 1.7 Hz), 7.65-7.71 (11H, m), 4.63 (1H, s), 1.43 (72H, s); ^{13}C NMR (150 MHz, $CDCl_3$) δ 149.6, 149.0, 148.3, 144.9, 143.7, 142.7, 142.5, 140.7, 139.4, 133.8, 133.5, 132.5, 132.4, 130.9, 128.8, 127.8, 127.4, 126.9, 124.4, 121.4, 121.3, 120.8, 96.0, 95.1, 87.5, 66.6, 35.0, 31.6; *m/z* (MALDI-TOF, +ve) 1820.9 (100%), 1836.9 (51%) ($C_{119}H_{115}N_9Ni_2O_3$ requires 1836.8, -OH requires 1819.8)

.

5c (X = OMe) :

Methoxy substituted dimer **5c** was synthesized by a similar procedure as that for **5a**. Acetylene porphyrin **4** (0.050 g, 0.059 mmol) and methyl *p*-methoxybenzoate (0.0049 g, 0.03 mmol) were dissolved in dry THF (1 mL) and cooled to −78°C. Lithium bis(trimethylsilyl)amide (1.0 M in THF, 0.24 mL, 0.24 mmol) was added to the above solution. The reaction mixture was allowed to warm to room temperature and stirred for 1 hr, after which the reaction was quenched with aqueous ammonium chloride (1 mL). The product was extracted with CH_2Cl_2 (30 mL) and washed with H_2O (3 × 20 mL), before passing through a short silica plug (CH_2Cl_2). The product was purified by column chromatography (2:1 40-60°C Petroleum ether / CH_2Cl_2). Removal of the solvent gave the product **5c** as a red solid (0.020 g, 38 % yield).

^{1}H NMR (400 MHz, $CDCl_3$) δ 9.63 (4H, d, *J* = 4.8 Hz), 8.82 (4H, d, *J* = 4.8 Hz), 8.70 (8H, m), 8.51 (2H, d, *J* = 8.9 Hz), 8.00 (4H, d, *J* = 7.3 Hz), 7.82 (8H, d, *J* = 1.9 Hz), 7.65-7.71 (11H, m), 3.94 (1H, s), 3.93 (1H, s), 1.44 (72H, s); *m/z* (MALDI-TOF, +ve) 1805.6 (100%), 1821.7 (30%) ($C_{120}H_{118}N_8Ni_2O_2$ requires 1821.8, -OH requires 1804.8).

Reference monomer **6**

Reference monomer **6** was synthesized by a similar procedure as that for **5a**. Acetylene porphyrin **4** (0.046 g, 0.055 mmol) and benzophenone (0.010 g, 0.059 mmol) were dissolved in dry THF (1 mL) and cooled to −78°C. Lithium bis(trimethylsilyl)amide (1.0 M in THF, 0.24 mL, 0.24 mmol) was added to the above solution. The reaction mixture was allowed to warm to room temperature and stirred for 1 hr, after which the reaction was quenched with aqueous ammonium chloride (1 mL). The product was extracted with CH_2Cl_2 (30 mL) and washed with H_2O (3 × 20 mL), before passing through a short silica plug (CH_2Cl_2). The product was purified by column chromatography (2:1 40-60°C Petroleum ether / CH_2Cl_2). Removal of the solvent gave the product **6** as a red solid (0.035 g, 60 % yield). λ_{max} ($CHCl_3$) / nm (log ε) 427 (5.43), 541 (4.25), 574 (3.95); ^{1}H NMR (400 MHz, $CDCl_3$) δ 9.48 (2H, d, *J* = 4.9 Hz), 8.86 (2H, d, *J* = 4.9 Hz), 8.75 (2H, d, *J* = 4.9 Hz), 8.73 (2H, d, *J* = 4.9 Hz), 8.03 (6H, m), 7.88 (4H, d, *J* = 1.9 Hz), 7.77 (2H, t, *J* = 1.9 Hz), 7.66-7.71 (3H, m), 7.51 (4H, t, *J* = 7.5 Hz), 7.41 (2H, t, *J* = 7.5 Hz), 3.32 (1H, s), 1.51 (36H, s); ^{13}C NMR (125 MHz, $CDCl_3$) δ 149.0, 145.3, 145.0, 143.5, 142.7, 142.5, 140.8, 139.6, 133.5, 133.5, 132.4, 132.3, 131.2, 128.8, 128.6, 128.0, 127.8, 126.9, 126.3, 121.3, 121.2, 120.5, 98.7, 97.4, 88.2, 75.8, 35.0, 31.7; *m/z* (MALDI-TOF, +ve) 1026.4 (100%), 1009.4 (91%) ($C_{69}H_{66}N_4NiO$ requires 1024.5, -OH requires 1007.5

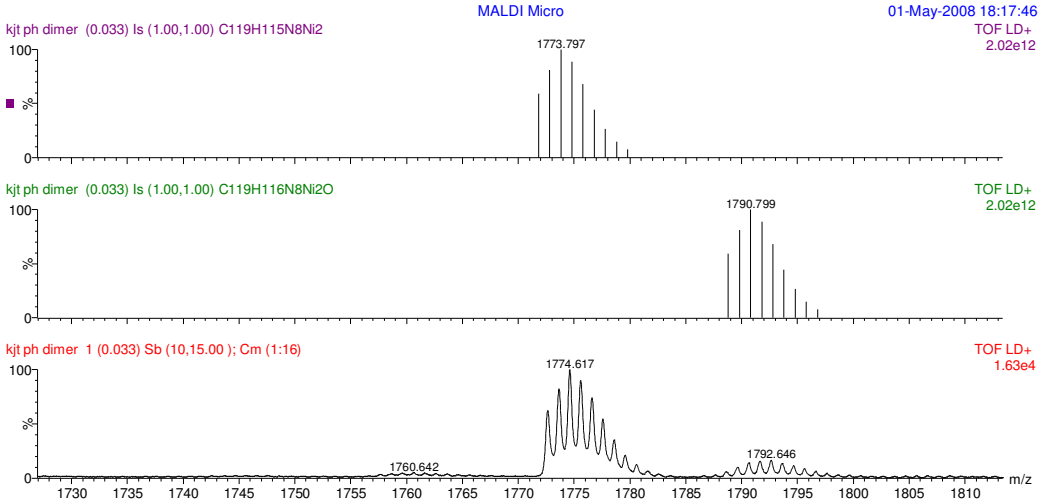

Figure S3. MALDI-TOF spectra of porphyrin monomer **6** using a dithranol matrix. Calculated isotopic patterns for porphyrin **6** (middle) and cation **7** (top) for reference.

Cationic porphyrin dimers **1a-c** and monomer **7**

Cationic porphyrins **1a-c** and **7** were formed *in situ* for NMR and absorption spectra measurements. A known amount of the porphyrin precursor **5a-c** or **6** was dissolved in chloroform and trifluoroacetic acid (2% by volume) was added.

1a (X = H):

λ_{max} ($CHCl_3$ / 2% TFA) / nm (log ε) 423 (5.12), 537 (4.70), 745 (4.08), 1240 (5.21); ^{1}H NMR (400 MHz, $CDCl_3$ / 2% *d*-TFA) δ 9.21 (4H, d, *J* = 4.9 Hz), 8.71 (2H, m), 8.60 (4H, d, *J* = 4.9 Hz), 8.25 (4H, d, *J* = 5.0 Hz), 8.20 (4H, d, *J* = 5.0 Hz), 7.95 (2H, d, *J* = 4.7 Hz), 7.87 (4H, d, *J* = 7.9 Hz), 7.80 (4H, t, *J* = 1.8 Hz), 7.69-7.74 (15H, m), 1.50 (72H, s); 13C NMR (150 MHz, $CDCl_3$ / 2% *d*-TFA) δ 155.3, 150.1, 148.6, 147.6, 144.2, 143.9, 143.5, 142.4, 138.3, 137.4, 136.3, 136.1, 134.6, 133.9, 132.9, 132.5, 131.0, 130.4, 130.1, 129.4, 127.7, 127.5, 122.5, 118.9, 96.4, 35.0, 31.5

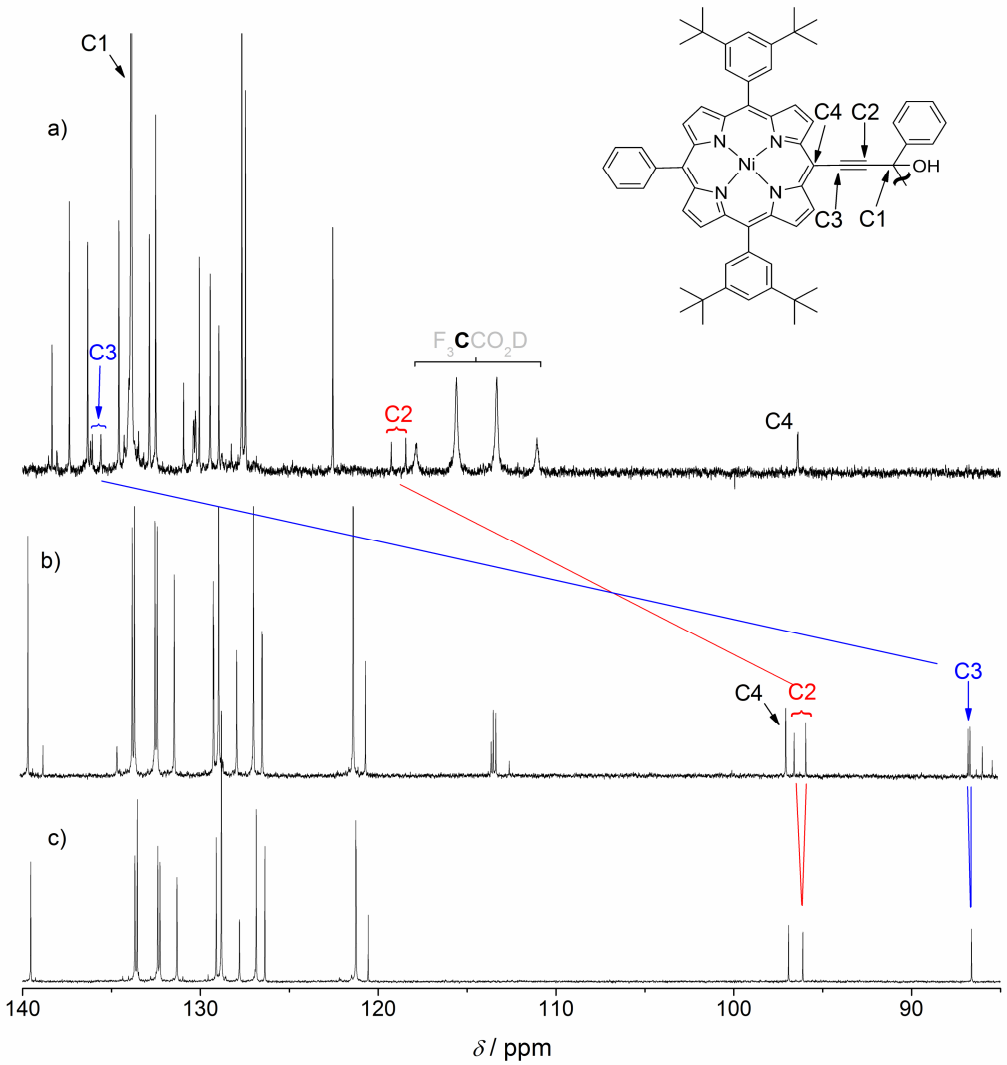

Figure S4. ^{13}C NMR spectra recorded at 125 MHz at 298 K of a) ^{13}C labeled cationic dimer **1a** in $CDCl_3$ / 2% *d*-TFA, b) ^{13}C labeled dimer **5a** in $CDCl_3$ and c) natural abundant dimer **5a** in $CDCl_3$. The C1 peaks in spectra b) and c) occur at 67.6 ppm. The signals for C2 and C3 can be distinguished by their coupling constants to the labeled C1 carbon.

1b (X = NO_2):

λ_{max} ($CHCl_3$ / 2% TFA) / nm (log ε) 421 (5.05), 537 (4.71), 1348 (5.10);

1c (X = OMe):

λ_{max} ($CHCl_3$ / 2% TFA) / nm (log ε) 421 (5.23), 532 (4.83), 774 (4.52), 1176 (5.06);

Monomer **7**

λ_{max} ($CHCl_3$ / 2% TFA) / nm (log ε) 388 (4.80), 526 (4.86), 824 (4.80), 1000 (4.11); ^1H NMR (400 MHz, $CDCl_3$ / 2% *d*-TFA) δ 8.51 (2H, d, *J* = 4.9 Hz), 8.18 (2H, d, *J* = 4.9 Hz), 8.09 (4H, d, *J* = 7.4 Hz), 7.90 (2H, t, *J* = 7.4 Hz), 7.84 (2H, d, *J* = 4.9 Hz), 7.72-7.80 (10H, m), 7.69 (1H, t, *J* = 7.4 Hz), 7.64 (2H, t, *J* = 7.5 Hz), 7.57, (4H, m), 1.46 (36H, m); ^{13}C NMR (150 MHz, $CDCl_3$ / 2% *d*-TFA) δ 163.6, 160.8, 150.8, 150.5, 149.8, 145.2, 144.3, 138.1, 137.6, 137.2, 136.6, 136.1, 136.0, 135.4, 135.3, 133.0, 132.7, 131.8, 130.1, 129.4, 129.0, 127.7, 126.6, 123.3, 99.1, 35.0, 31.4

Section 2. Nonlinear Optical Characterization Techniques.

The laser source used was a regeneratively amplified Ti:Sapphire system (Spitfire, Spectra-Physics) which, in turn, pumped an optical parametric amplifier (TOPAS-c, Spectra-Physics) whose signal beam generates ~100 fs pulses at 1550 nm with a repetition rate of 1 kHz. The solutions used for the nonlinear characterization experiments were contained in 1 mm glass cuvettes and had concentrations of ~$1x10^{-3}$ M. Typically solutions of **5a** were prepared in $CHCl_3$ beforehand and prior to nonlinear characterization 2% of TFA was added to a portion of the solution to produce **1a**.

The optical layout for the *Z*-scan technique was a standard one.[6] Detection of the reference, open-aperture and closed-aperture signals were performed using large area Germanium photoreceivers (2033, New Focus). These signals were passed through Boxcar integrator units (SR250, Stanford Research Systems) and the processed signals were acquired using a data acquisition card (6025E, National Instruments) and a home-built Labview program. *Z*-scans were performed using excitation irradiances that ranged from 10 – 150 GW/cm^2. While open-aperture scans on the chromophores in solution permitted direct determination of the imaginary component of the second-order hyperpolarizability, γ, determination of the Re(γ) required closed-aperture scans on both the solution as well as the neat solvent. This permitted subtraction of the signal due to the neat solvent from the solution to determine the contribution of the solute alone. The nonlinearities were extracted by applying theoretical curve fittings to the experimental data as described in Reference 6. These curve fittings are based upon the assumption that the nonlinearity is purely third-order in its origin. The data can be fit quite well under this assumption. Open aperture data (see Figure 3b) are slightly broader than the fitting curves due to the presence of saturation as observed in the transient absorption measurements (see Figure S6). As further evidence for a third-order nonlinearity, the extracted values for γ were found to be independent of excitation irradiance. Also, power-dependent DFWM signals show a cubic response (see Figure S5) further suggesting a third-order nonlinearity. Finally, it should be noted that in order to eliminate thermal effects that could potentially obscure the closed-aperture results,[7] the repetition rate of the system was reduced to 50 Hz. This was found to reduce the thermal contributions to the closed-aperture signals to a negligible level.

The degenerate four-wave mixing (DFWM) layout was a standard forward-scattering or folded-boxcars geometry[4] with angular beam separation of ~1.5°. The signal and reference beams were detected in a similar manner to that described above. Thermal nonlinearities were not found to obscure the DFWM signals even at the 1 kHz repetition rate. The irradiance-dependent response of the DFWM signal was determined by monitoring the signal beam while the energies of the inputs beams were varied using a computer-controlled attenuator. Figure S5 shows the intensity-dependent response of the DFWM signal for a number of different samples. The data for both fused silica and $CHCl_3$ are fit quite well to the linear curves with slopes of three, as expected for a non-resonant third-order nonlinearity. The DFWM signal for **1a** also shows reasonable agreement to a cubic response especially at lower intensities. The response becomes slightly hypocubic at higher intensities as a result of increased nonlinear absorption resulting in reduced driving intensities. The temporal response of the DFWM signal was determined by monitoring the signal beam while translating one of the three pump pulses through the use of a computer-controlled delay line.

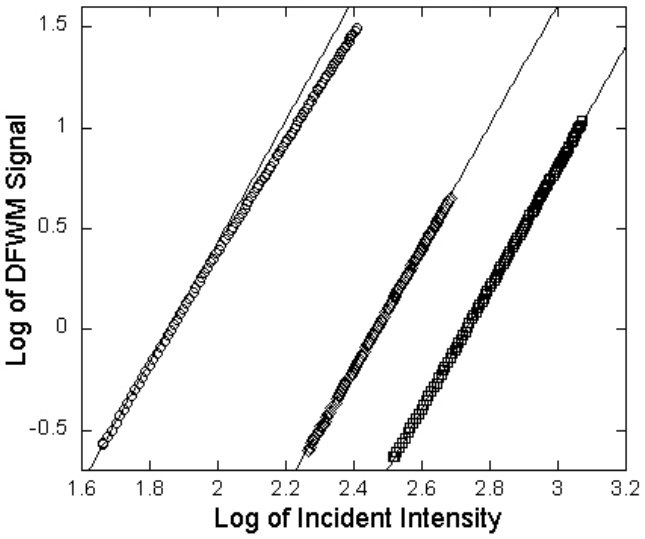

Figure S5. Intensity-dependent response of DFWM signals for a 1 mm slab of fused silica (squares) and for 1 mm cuvettes containing both $CHCl_3$ (diamonds) and **1a** in $CHCl_3$ / 2% TFA (circles). The solid curves are lines with slopes of 3 generated for comparison with the experimental data.

Figure S6 shows the transient absorption temporal response at 1550 nm for the solution of **1a**. The transient absorption optical layout was identical to the DFWM layout with one of the three beams blocked. By monitoring one of the remaining two beams while translating its associated pulse using the delay line, the temporal response of the transient absorption could be determined. The ultrafast induced absorption component is caused by two photon absorption (similar to open aperture *Z*-scan) while the saturation component (similar lifetime to that found by TR-DFWM) likely results from a smaller excited-state absorption cross-section compared to ground-state cross-section at this wavelength.

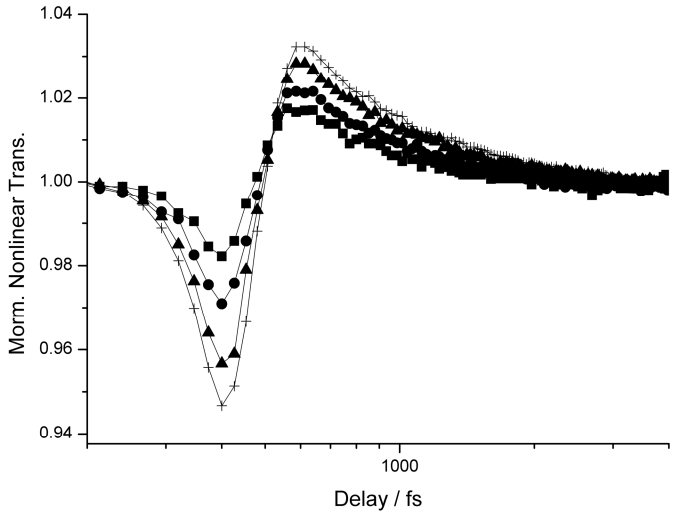

Figure S6. Transient absorption signals performed at 1550 nm for **1a** in $CHCl_3$ / 2% TFA using different excitation irradiances.

Section 3. Comparison of Effective Delocalization Lengths.

Comparison of the nonlinearity and position of the absorption maxima of the bis-porphyrin cation **1a** and the bis-dioxaborine cyanine reported previously[8] **2** provides an estimate of the effective delocalization lengths. The nearly linear dependence of the electronic absorption maximum (λ) with number of bonds (N) for simple polymethine cyanines has long been known[9] and can be determined by the following:[10]

$$\lambda_{\max} = \frac{8 \cdot m \cdot c}{h} * \frac{(N \cdot l)^2}{N+1} \qquad (1)$$

where m is the mass of the electron, c is the speed of light, h is Planck's constant, and l is the average bond length along the conjugated chain, taken to be 1.36 Å.[11] Using Eq. (1), one can estimate the effective conjugation length over which delocalization occurs for the bis-dioxaborine cyanine **2** to be ~16 bonds ($\lambda_{\max}^{\text{calc}}$ = 918 nm; $\lambda_{\max}^{\text{meas}}$ = 942 nm) as compared to a linear edge-to-edge length of ~14 bonds for the molecule without accounting for the effect of the fused benzene ring at the terminal positions. Interestingly, the effective conjugation length for the bis-porphyrin cation **1a** is estimated to be ~ 22 bonds based on $\lambda_{\max}$ ($\lambda_{\max}^{\text{calc}}$ = 1283 nm; $\lambda_{\max}^{\text{meas}}$ = 1243 nm), compared to a linear physical length of ~18 bonds, not considering the *meso*-phenyl groups. The discrepancy between the calculated conjugation-length values and the actual physical lengths can be attributed to increased delocalization provided by these terminal groups. However, without further evidence of the degree to which charge is delocalized over these terminal moieties, a conservative approach suggests that the physical lengths provide a reasonable estimation of the conjugation lengths over which delocalization exists. It is also known that the third-order polarizability of cyanines follows a power law dependence on the number of conjugated bonds (N): $\gamma \propto N^{\alpha}$ where α ranges from 7 to 9.[11] Taking α to be 7, allows one to estimate the ratio of conjugation lengths for the bis-porphyrin cation **1a** relative to the bis-dioxaborine cyanine **2**. From the ratio of γ values the relative length (bis-porphyrin to bis-dioxaborine) is 1.28, whereas the ratio of physical lengths from a structural model is 1.29 (18/14) and that from the relative lengths obtained from the $\lambda_{\max}$ data is 1.38 (22/16), all of which are reasonably consistent and indicative of a similar degree of delocalization but over a greater length for the bis-porphyrin cation **1a** compared to the bis-dioxaborine cyanine **2**.

Section 4. References

[1] M. O. Senge, *Acc. Chem. Res.* **2005**, *38*, 733-743.

[2] S. G. DiMagno, V. S.-Y. Lin, M. J. Therien, *J. Org. Chem.* **1993**, *58*, 5983-5993.

[3] M. J. Plater, S. Aitken, G. Bourhill, *Tetrahedron* **2002**, *58*, 2405-2413.

[4] S. M. Kuebler, R. G. Denning, H. L. Anderson, *J. Am. Chem. Soc.* **2000**, *122*, 339-347.

[5] W. M. Weber, L. A. Hunsaker, S. F. Abcouwer, L. M. Deck, D. L. V. Jagt, *Bioorg. Med. Chem.* **2005**, *13*, 3811-3820.

[6] M. Sheik-Bahae, A. A. Said, E. W. V. Stryland, *Opt. Lett.* **1989**, *14*, 955-957.

[7] A. Gnoli, L. Razzari, M. Righini, *Optics Express* **2005**, *13*, 7976-7981.

[8] J. M. Hales, S. Zheng, S. Barlow, S. R. Marder, J. W. Perry, *J. Am. Chem. Soc.* **2006**, *128*, 11362-11363.

[9] H. Kuhn, *J. Chem. Phys.* **1949**, *17*, 1198-1212.

[10] In the original paper, the N term in the denominator of Eq. (1) was actually given as the number of π-electrons along the conjugated chain. However, for the simple nitrogen-terminated polymethine cyanines discussed therein, this value is equivalent to the number of bonds in the conjugated chain.

[11] J. L. Bredas, C. Adant, P. Tackx, A. Persoons, B. M. Pierce, *Chem. Rev.* **1994**, *94*, 243-278.